NeuroImage: Clinical 24 (2019) 102019

Contents lists available at ScienceDirect

NeuroImage: Clinical

journal homepage: www.elsevier.com/locate/ynicl

Brain structural connectivity network alterations in insomnia disorder reveal a central role of the right angular gyrus

Yishul Wei[a], Tom Bresser[a,b,c], Rick Wassing[a,d], Diederick Stoffers[e], Eus J.W. Van Someren[a,c,f,*,†], Jessica C. Foster-Dingley[a,†]

[a] Department of Sleep and Cognition, Netherlands Institute for Neuroscience (NIN), an Institute of the Royal Netherlands Academy of Arts and Sciences, Amsterdam, The Netherlands
[b] Dutch Connectome Lab, Department of Complex Trait Genetics, Center for Neurogenomics and Cognitive Research (CNCR), Amsterdam Neuroscience, VU University Amsterdam, Amsterdam, The Netherlands
[c] Department of Integrative Neurophysiology, Center for Neurogenomics and Cognitive Research (CNCR), Amsterdam Neuroscience, VU University Amsterdam, Amsterdam, The Netherlands
[d] Centre for Integrated Research and Understanding of Sleep (CIRUS), Woolcock Institute of Medical Research, University of Sydney, Sydney, Australia
[e] Spinoza Centre for Neuroimaging, Amsterdam, The Netherlands
[f] Amsterdam UMC, Vrije Universiteit, Psychiatry, Amsterdam Neuroscience, Amsterdam, The Netherlands

ARTICLE INFO

Keywords:
Tractography
Diffusion-weighted MRI
Connectome
Angular gyrus
Insomnia disorder
Reactivity

ABSTRACT

Insomnia Disorder (ID) is a prevalent and persistent condition, yet its neural substrate is not well understood. The cognitive, emotional, and behavioral characteristics of ID suggest that vulnerability involves distributed brain networks rather than a single brain area or connection. The present study utilized probabilistic diffusion tractography to compare the whole-brain structural connectivity networks of people with ID and those of matched controls without sleep complaints.

Diffusion-weighted images and T1-weighed images were acquired in 51 people diagnosed with ID (21–69 years of age, 37 female) and 48 matched controls without sleep complaints (22–70 years of age, 31 female). Probabilistic tractography was performed to construct the whole-brain structural connectivity network of each participant. Case–control differences in connectivity strength and network efficiency were evaluated with permutation tests.

People with ID showed structural hyperconnectivity within a subnetwork that spread over frontal, parietal, temporal, and subcortical regions and was anchored at the right angular gyrus. The result was robust across different edge-weighting strategies. Moreover, converging support was given by the finding of heightened right angular gyrus nodal efficiency (harmonic centrality) across varying graph density in people with ID. Follow-up correlation analyses revealed that subnetwork connectivity was associated with self-reported reactive hyperarousal.

The findings demonstrate that the right angular gyrus is a hub of enhanced structural connectivity in ID. Hyperconnectivity within the identified subnetwork may contribute to increased reactivity to stimuli and may signify vulnerability to ID.

ANTs	Advanced Normalization Tools
CON	cingulo-opercular network
DMN	default-mode network
DWI	diffusion-weighted imaging
EPI	echo-planar imaging
FCN	frontoparietal control network
FDT	FMRIB's Diffusion Toolbox
FSL	FMRIB's Software Library
HAS	Hyperarousal Scale
ID	Insomnia Disorder
ISI	Insomnia Severity Index
MNI	Montreal Neurological Institute
MRI	magnetic resonance imaging
NBS	network-based statistic

* Corresponding author at: Department of Sleep and Cognition, Netherlands Institute for Neuroscience (NIN), an Institute of the Royal Netherlands Academy of Arts and Sciences, Meibergdreef 47, Amsterdam 1105 BA, The Netherlands.
E-mail address: e.j.w.someren@vu.nl (E.J.W. Van Someren).
† Both authors contributed equally.

https://doi.org/10.1016/j.nicl.2019.102019
Received 15 May 2019; Received in revised form 5 August 2019; Accepted 27 September 2019
Available online 22 October 2019

SyN Symmetric Normalization
VAN ventral attention network

1. Introduction

With an estimated prevalence of about 10%, Insomnia Disorder (ID) is the most prevalent sleep disorder, and its prevalence has kept rising in industrialized countries (Chaput et al., 2018; Riemann et al., 2017). Longitudinal studies have shown that insomnia predicts incidences of diabetes (Cappuccio et al., 2010), cardiovascular diseases (He et al., 2017; Sofi et al., 2014), dementia (Shi et al., 2018), chronic pain (Andersen et al., 2018), and mental disorders (Hertenstein et al., 2019). Accumulating evidence suggests that management of insomnia is of value for the prevention and amelioration of these conditions (Kyle and Henry, 2017; Smith et al., 2005; Wu et al., 2015; Wulff et al., 2010). The central role of insomnia particularly in the psychiatric symptom network (Borsboom et al., 2011) highlights sleep as a promising transdiagnostic target in mental healthcare (Dolsen et al., 2014; Harvey et al., 2011). However, the neurobiological basis of insomnia remains elusive (Tahmasian et al., 2018), which has hampered progress in developing novel, effective interventions.

ID is characterized by not only sleep complaints but also complaints about daytime functions including attention, memory, executive functioning, and mood (Edinger et al., 2004; Morin et al., 2015). The fact that the complaints of people with ID span many domains of brain functions suggests that its pathology involves multiple brain areas and connections across large-scale brain networks (Medaglia et al., 2015; Park and Friston, 2013). Diffusion-weighted imaging (DWI) is a magnetic resonance imaging (MRI) technique that enables the study of brain structural connectivity *in vivo*. Based on information provided by DWI about water diffusion within each voxel, white matter fiber trajectories can be constructed through computational algorithms generally known as tractography (Jeurissen et al., 2019). In the present study, we utilized probabilistic diffusion tractography with the aim of detecting brain structural connectivity alterations that could underlie the diverse complaints of people with ID.

Whole-brain tractography produces millions of estimated fiber trajectories (streamlines) which are typically integrated into a coarse-grained network and subsequently studied with graph theory or other network-based analyses (Bullmore and Sporns, 2009; Park and Friston, 2013; Sotiropoulos and Zalesky, 2019). The nodes in the coarse-grained structural connectivity network represent macroscopic brain regions. The edges in the network denote connections between pairs of these regions, with the weight of each edge corresponding to some measure of "connectivity strength". However, precisely how the edge weights should be calculated from tractography output has been a topic of discussion, and to date there is no gold standard (Buchanan et al., 2014; Dimitriadis et al., 2017; Messaritaki et al., 2019; Roine et al., 2019). For this reason, we consider it best practice to apply a range of edge-weighting strategies and verify the robustness of results across these strategies.

To our knowledge, two studies have investigated the whole-brain structural connectivity networks of people with ID as compared to those of people without sleep complaints using tractography. One study reported abnormalities associated with ID in the limbic cortico-basal-ganglia circuit and the default-mode network (Wu et al., 2018). The other study reported reduced connectivity strength in ID among the left insular, frontal, and subcortical regions (Jespersen et al., 2019). Limitations of the former study included an unfavorable signal-to-noise ratio owing to the 1.5-Tesla MRI hardware (Hunsche et al., 2001; Okada et al., 2007), while the latter study was limited by the relatively small sample size of 16 people with ID and 14 matched controls. Furthermore, neither of the two studies addressed whether the results were robust across different edge-weighting strategies. The present study thus undertook special efforts to overcome the methodological limitations of these previous studies, specifically by recruiting an adequate number of participants and by reporting findings that are consistent across several edge-weighting strategies. We performed both graph theory (Bullmore and Sporns, 2009) and network-based statistic (Zalesky et al., 2010) analyses in order to gain detailed insights into the brain structural connectivity alterations in ID.

2. Methods

Assessments were part of more elaborate studies which were approved by the Ethics Review Board of the University of Amsterdam. All participants provided written informed consent.

2.1. Participants

Participants were recruited through advertisement and the Netherlands Sleep Registry and were screened by telephone followed by a face-to-face structured interview. Participants meeting the diagnostic criteria for Insomnia Disorder (American Academy of Sleep Medicine, 2014; American Psychiatric Association, 2013) were included in the ID group ($n = 51$, age range 21–69 years). The control group consisted of age- and sex-matched volunteers that reported to have no sleep difficulties ($n = 48$, age range 22–70 years). Exclusion criteria for all participants were: (1) diagnosed current or past neurological or psychiatric disorders other than ID; (2) current sleep disorders other than ID; (3) shift work; (4) use of sleep medications within the prior 2 months; (5) MRI contraindications such as MR-incompatible metal implants, claustrophobia, or pregnancy. Brief self-reported measures including the Insomnia Severity Index (ISI) (Bastien et al., 2001) and the shortened Hyperarousal Scale (HAS) (Pavlova et al., 2001; Wassing et al., 2016) were administered during intake. Table 1 summarizes the demographic characteristics of the participants as well as their self-reported insomnia duration, insomnia severity as assessed by the ISI, and hyperarousal traits as assessed by the sum score and 2 subscales of the HAS (Pavlova et al., 2001).

2.2. MRI protocol

Participants were scanned on 3-Tesla MRI scanners of the same brand and type (Achieva, Philips Medical Systems, Best, The Netherlands) with 32-channel head coils at 2 different sites of the Spinoza Centre for Neuroimaging, Amsterdam, The Netherlands. On the assessment days, participants were asked to refrain from alcohol and drugs. Participants were not allowed to consume caffeinated beverages for at least 6 h before the MRI scanning sessions. Scans were made between 9:00 and 20:00 h. Diffusion-weighted images were acquired from an isotropic single-shot echo-planar imaging (EPI) spin echo sequence with 32 non-collinear diffusion gradient directions ($b = 1000$ s/mm^2) along with 1 non-diffusion-weighted volume ($b = 0$ s/mm^2). The scanning parameters were: repetition time = 16 s, echo time = 48 ms,

Table 1
Characteristics of the Participants (mean ± standard deviation).

	Control ($n = 48$)	Insomnia Disorder ($n = 51$)	p
Age (y)	44.5 ± 15.0	48.0 ± 14.4	0.27
Sex (female/male)	31/17	37/14	0.52
Insomnia Duration (y)	—	20.2 ± 15.2	—
ISI	3.9 ± 4.1	16.6 ± 5.0	1.3×10^{-15}
HAS	19.5 ± 7.0	23.0 ± 8.2	0.01
HAS-Introspectiveness	10.9 ± 3.7	12.5 ± 4.5	0.03
HAS-Reactivity	3.8 ± 2.5	4.3 ± 2.5	0.19

ISI, Insomnia Severity Index; HAS, Hyperarousal Scale (shortened version as used in Wassing et al. (2016)).
p-values are determined by Fisher exact test for sex and by Wilcoxon rank-sum tests for the other variables.

phase-encoding direction = AP, flip angle = 90°, field of view = 224 × 224 × 130 mm^3 (AP × RL × FH), voxel size = 2 × 2 × 2 mm^3, slice gap = 0 mm, SENSE factor = 3 (AP). Additionally, T1-weighted images were acquired from a 3D Turbo Field Echo sequence with the following scanning parameters: repetition time = 8.3 ms, echo time = 3.8 ms, phase-encoding direction = RL, flip angle = 8°, field of view = 240 × 188 × 220 mm^3 (AP × RL × FH), voxel size = 1 × 1 × 1 mm^3, SENSE factors = 2.5 (RL), 2 (FH).

2.3. Image preprocessing

FMRIB's Software Library (FSL) version 5.0.10 was used to preprocess imaging data (Smith et al., 2004). Distortions in the diffusion-weighted images due to motion and eddy currents were corrected by the *eddy* program in FMRIB's Diffusion Toolbox (FDT) with outlier replacement (Andersson et al., 2016; Andersson and Sotiropoulos, 2016). Fiber orientation distribution functions were estimated from the diffusion-weighted images by the *bedpostx* program in FDT, which uses a Bayesian method with automatic relevance determination to infer a multi-fiber partial volume model for each voxel (Behrens et al., 2007). Visual quality checking of all images was conducted with FSLView.

2.4. Network construction

The 94 cortical and subcortical parcels (excluding the cerebellum) in the AAL2 atlas were taken as network nodes (Rolls et al., 2015). We registered the Montreal Neurological Institute (MNI) high-resolution single-subject T1-weighted image (viz. colin27, on which the AAL2 atlas is delineated) to each participant's T1-weighted image using the nonlinear Symmetric Normalization (SyN) algorithm implemented in the Advanced Normalization Tools (ANTs) version 2.1.0 (Avants et al., 2008, 2011). As small geometric distortions could still be observed in the preprocessed diffusion-weighted images relative to the T1-weighted images, we also ran nonlinear SyN to co-register the 2 modalities (Wang et al., 2017). The nonlinear transformations were concatenated so as to register the AAL2 parcels to individual DWI spaces. All registration results were visually inspected to ensure adequate alignment.

Probabilistic tractography was performed by the *probtrackx2* program in FDT. Fiber tracking was carried out in native DWI spaces. The 94 SyN-transformed AAL2 parcels were assigned as both seeding and stopping masks, and 5000 seeds were set to propagate from each voxel within the seeding masks. Voxels with principal anisotropic volume fraction ($f1$ estimated by *bedpostx*) below 0.05 were masked out to avoid tracking into regions with highly uncertain fiber orientations (mainly cortical gray matter and cerebrospinal fluid-filled cavities).

All subsequent analyses were conducted in MATLAB 8.3 (The Mathworks Inc., Natick, Massachusetts, United States). The whole-brain structural connectivity network of each participant can be numerically represented as a 94 × 94 matrix of "connectivity strength" values. For the main results reported hereafter, we used the number of probabilistic streamlines connecting a pair of regions, divided by the total number of seeds propagating from the 2 regions (i.e., 5000 times the number of voxels), as the measure of connectivity strength between the 2 regions (equivalent to the edge weights used in some previous works (Li et al., 2012; Owen et al., 2013)). This can be conceptually understood as the capacity of direct information exchange per unit volume between the 2 regions (with each seed interpreted as 1 "unit of information"). Other edge-weighting schemes are outlined in the Supplementary Material.

2.5. Between-group statistical comparisons

We first examined overall and regional topology of the structural connectivity networks according to global, local, and nodal efficiency indices, which are among the most widely studied network descriptors in network neuroscience and are closely linked to other graph-theoretical concepts such as path length, clustering, and centrality (Bullmore and Sporns, 2009). Moreover, network efficiency can be intuitively understood under the principles of "economical" network organization, i.e., in terms of the trade-offs between wiring costs and information integration (Achard and Bullmore, 2007; Bullmore and Sporns, 2012). Here we followed the framework laid out by Achard and Bullmore (2007), who used graph density as the operationalization of wiring costs. Graph density is controlled by setting a connectivity strength threshold and keeping only edges with weights above the threshold in the network. One can then study the trade-offs between wiring costs and information integration by scrutinizing how efficiency indices change with graph density. Global, local, and nodal efficiency indices measure different aspects of information integration (Achard and Bullmore, 2007): First, global efficiency, defined as the inverse harmonic mean of all pairwise shortest path lengths between nodes, signifies the capacity of parallel information exchange over the whole network. Second, local efficiency is obtained by averaging efficiency computed on each local subgraph (which consists of a node's immediately adjacent nodes). It quantifies efficiency of information exchange at the local level when a node is removed, which can be though of as fault tolerance. Third, nodal efficiency (also known as harmonic centrality) is the contribution of each node to global efficiency and signifies how central a node is in the information network.

Following this framework, we computed the efficiency indices for graph density levels between 1% and 40% in steps of 1%, thus covering a wide range of density levels considered in other studies. We evaluated significance of group differences consistent across varying graph density with permutation tests, as follows. The efficiency indices for each density level were first compared between the groups by means of Wilcoxon rank-sum tests. The rank-sum Z-values were then summed over all density levels to obtain the final test statistics for group differences. Next, the same test statistics were computed with the participants' group membership labels randomly shuffled. This was repeated 10,000 times to construct a null randomization distribution of each test statistic. (For nodal efficiency, only a null randomization distribution of the maximum absolute value across all nodes was constructed, to account for multiple comparisons.) Finally, significance of group differences across varying graph density was determined by comparing the real observed values of the test statistics against the corresponding null distributions.

To gain more detailed insights into group differences in brain structural connectivity, we also performed edge-wise Wilcoxon rank-sum tests on connectivity strength and used network-based statistic (NBS) to control the overall false positive rate. In brief, NBS involves setting a Z-value threshold and assessing statistical significance of sizes of supra-threshold subnetworks (connected components) through a permutation procedure (Zalesky et al., 2010). To ascertain that inference was consistent across a reasonably wide range of cluster-forming Z-value thresholds, we ran NBS multiple times with the Z-value threshold varying from 2.5 to 3.0 in steps of 0.1. For each Z-value threshold, 10,000 randomization iterations were used to construct a null distribution of the test statistic (size of the largest supra-threshold connected component) and deduce the final p-value.

2.6. Follow-up correlation analyses

We conducted follow-up correlation analyses to evaluate whether subnetwork structural connectivity was associated with self-reported trait measures. Each edge weight was first standardized with respect to the mean and standard deviation of the control group. (The standardized edge weight thus quantifies how much connectivity strength for a particular edge in one participant deviates from the controls' mean.) A summary subnetwork connectivity score for each participant was then derived by summing the standardized edge weights over the largest supra-threshold connected component described above with Z-value threshold = 3.0. Spearman correlation coefficients between

subnetwork connectivity and trait measures were computed across all participants.

Within the ID group, we also assessed the Spearman correlation coefficient between subnetwork structural connectivity and insomnia duration. A critical question regarding case–control difference findings in clinical neuroimaging studies is whether specific deviations in patients predispose to the development of the disorder or rather are the results of having been exposed to the disorder. In the latter case, longer exposure would be expected to be associated with larger deviations. Conversely, a lack of association with disorder duration would hint that the deviations rather indicate vulnerability to the disorder.

3. Results

3.1. Between-group network differences

People with ID did not significantly differ from controls in terms of global efficiency (permutation test: $p = 0.38$) or local efficiency (permutation test: $p = 0.53$) across varying graph density. Even with a lenient significance criterion of $p < 0.05$ at single density levels without correction for multiple comparisons, no significant group difference in global efficiency could be observed (Wilcoxon rank-sum tests: $-1.50 < Z < 1.76$ for all density levels between 1% and 40%), while significant group differences in local efficiency were observed only within a small range of density levels between 37% and 39% (Wilcoxon rank-sum tests: $Z = 2.08$, 2.18, and 2.41 for density levels 37%, 38%, and 39%, respectively). This suggests that overall network topology in people with ID and controls exhibited largely similar economical small-world properties (Achard and Bullmore, 2007).

Despite the lack of group differences in overall network topology, there was evidence for region-specific alterations in ID. Nodal efficiency of the right angular gyrus was significantly higher in people with ID than in controls across varying graph density (permutation test: $p = 0.046$), indicating a more central role of the right angular gyrus in the whole-brain structural connectivity networks of people with ID. No other brain region had nodal efficiency significantly differing between the groups across varying graph density (permutation test: $p > 0.57$ for all nodes other than the right angular gyrus).

Further zooming in, we evaluated edge-wise group differences in connectivity strength with NBS. A single supra-threshold connected component with higher edge weights in ID was found to be significant for each cluster-forming Z-value threshold between 2.6 and 3.0 (Fig. 1), whereas a lower Z-value threshold of 2.5 yielded a supra-threshold connected component with a trend-level p-value of 0.057. For all cluster-forming Z-value thresholds, the right angular gyrus was a hub in the supra-threshold subnetwork with the highest degree. Table 2 lists the degree of each node as well as the edge-wise rank-sum Z-values within the subnetwork identified with Z-value threshold = 2.6. No subnetwork differing between the groups in the opposite direction (i.e., lower edge weights in ID) was found to be significant for any cluster-forming Z-value threshold.

All the other edge-weighting strategies we explored reproduced qualitatively similar subnetworks with increased connectivity strength in ID (Supplementary Material). Thus, the observed group differences were robust and depended only minimally on the choice of edge weights.

3.2. Associations with self-reported measures

Each participant's subnetwork connectivity was summarized by the standardized edge weight sum over the 7 edges visualized in the right panel of Fig. 1 (right angular gyrus – left middle cingulate gyrus, right angular gyrus – left posterior cingulate gyrus, right angular gyrus – left superior temporal gyrus, right angular gyrus – left middle temporal gyrus, right angular gyrus – left caudate nucleus, right angular gyrus – left putamen, and left putamen – left superior temporal gyrus). The correlation between subnetwork connectivity and the ISI across all participants was significant and positive (Spearman correlation coefficient $r_s(97) = 0.28$, $p = 0.005$). There was almost no correlation between subnetwork connectivity and the HAS sum score ($r_s(97) = 0.06$, $p = 0.58$). The correlation between subnetwork connectivity and the Introspectiveness subscale of the HAS was likewise almost nonexistent ($r_s(97) = -0.02$, $p = 0.86$). The Reactivity subscale of the HAS, on the other hand, was significantly and positively correlated with subnetwork connectivity ($r_s(97) = 0.23$, $p = 0.03$). Finally, within people with ID, subnetwork connectivity did not significantly correlate with insomnia duration ($r_s(49) = 0.10$, $p = 0.51$). Excluding the edge not incident to the right angular gyrus in the standardized edge weight sum reproduced the same correlation pattern with only minor numerical differences in the correlation coefficients.

4. Discussion

The current study compared the whole-brain structural connectivity networks of people with ID and those of matched controls without sleep complaints. NBS identified a subnetwork with increased connectivity strength in ID that spreads over frontal, parietal, temporal, and subcortical regions and is anchored at the right angular gyrus. Furthermore, deviated subnetwork connectivity is significantly associated with self-reported reactive hyperarousal in addition to insomnia severity. Graph theory corroborates the NBS result by singling out the right angular gyrus as being a more central node in the whole-brain structural connectivity networks of people with ID.

The angular gyrus belongs to the posterior heteromodal association cortex and is involved in a wide array of cognitive functions including attention, memory retrieval, conflict resolution, and theory of mind (Bzdok et al., 2013; Catani et al., 2017; Seghier, 2013). A framework proposed by Seghier (2013) hypothesizes that the angular gyrus interfaces bottom-up multisensory input with top-down predictions generated according to prior knowledge, learned experience, and agency. Based on the observed group differences, we propose that the cognitive complaints of people with ID could be partially attributed to altered

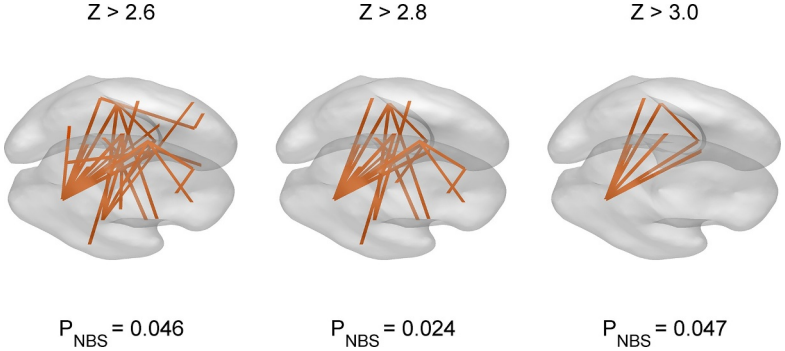

Fig. 1. Stronger brain structural connectivity in Insomnia Disorder. Edges with Wilcoxon rank-sum Z statistics above 2.6, 2.8, and 3.0 are depicted in the left, middle, and right panels, respectively. The p-value associated with each Z-value threshold as determined by network-based statistic (NBS) is shown at the bottom of each panel.

Table 2
The degree of each node in the $Z > 2.6$ subnetwork shown in Fig. 1 (i.e., number of each node's incident edges with increased connectivity strength in ID) and the associated edge-wise rank-sum Z-values.

Node	Degree	Adjacent Nodes	Z
Angular gyrus (R)	12	Middle cingulate gyrus (L)	3.91
		Caudate nucleus (L)	3.34
		Superior temporal gyrus (L)	3.30
		Putamen (L)	3.24
		Middle temporal gyrus (L)	3.06
		Posterior cingulate gyrus (L)	3.00
		Thalamus (L)	2.91
		Posterior cingulate gyrus (R)	2.90
		Supplementary motor area (R)	2.89
		Hippocampus (L)	2.80
		Precuneus (L)	2.68
		Insula (L)	2.61
Superior temporal gyrus (L)	4	Angular gyrus (R)	3.30
		Putamen (L)	3.01
		Insula (R)	2.89
		Supramarginal gyrus (R)	2.83
Supplementary motor area (R)	4	Anterior cingulate gyrus (R)	3.06
		Angular gyrus (R)	2.89
		Middle frontal gyrus (R)	2.82
		Supramarginal gyrus (R)	2.74
Supramarginal gyrus (R)	4	Superior temporal gyrus (L)	2.83
		Rolandic operculum (L)	2.81
		Inferior frontal gyrus, pars triangularis (L)	2.75
		Supplementary motor area (R)	2.74
Middle cingulate gyrus (L)	3	Angular gyrus (R)	3.91
		Middle temporal gyrus (R)	2.85
		Hippocampus (R)	2.69
Caudate nucleus (L)	3	Angular gyrus (R)	3.34
		Superior parietal gyrus (R)	2.68
		Medial orbitofrontal gyrus (L)	2.66
Hippocampus (L)	3	Paracentral lobule (R)	3.26
		Amygdala (R)	3.18
		Angular gyrus (R)	2.80
Putamen (L)	3	Angular gyrus (R)	3.24
		Superior temporal gyrus (L)	3.01
		Thalamus (R)	2.94
Anterior cingulate gyrus (R)	2	Supplementary motor area (R)	3.06
		Olfactory cortex (R)	3.00
Middle temporal gyrus (L)	2	Angular gyrus (R)	3.06
		Inferior frontal gyrus, pars orbitalis (L)	2.74
Inferior frontal gyrus, pars orbitalis (L)	2	Superior frontal gyrus (L)	2.86
		Middle temporal gyrus (L)	2.74
Paracentral lobule (R)	1	Hippocampus (L)	3.26
Amygdala (R)	1	Hippocampus (L)	3.18
Posterior cingulate gyrus (L)	1	Angular gyrus (R)	3.00
Olfactory cortex (R)	1	Anterior cingulate gyrus (R)	3.00
Thalamus (R)	1	Putamen (L)	2.94
Thalamus (L)	1	Angular gyrus (R)	2.91
Posterior cingulate gyrus (R)	1	Angular gyrus (R)	2.90
Insula (R)	1	Superior temporal gyrus (L)	2.89
Superior frontal gyrus (L)	1	Inferior frontal gyrus, pars orbitalis (L)	2.86
Middle temporal gyrus (R)	1	Middle cingulate gyrus (L)	2.85
Middle frontal gyrus (R)	1	Supplementary motor area (R)	2.82
Rolandic operculum (L)	1	Supramarginal gyrus (R)	2.81
Inferior frontal gyrus, pars triangularis (L)	1	Supramarginal gyrus (R)	2.75
Hippocampus (R)	1	Middle cingulate gyrus (L)	2.69
Superior parietal gyrus (R)	1	Caudate nucleus (L)	2.68
Precuneus (L)	1	Angular gyrus (R)	2.68
Medial orbitofrontal gyrus (L)	1	Caudate nucleus (L)	2.66
Insula (L)	1	Angular gyrus (R)	2.61

integration of bottom-up and top-down processes mediated by the hyperconnected right angular gyrus in line with this framework. The observed association between subnetwork structural connectivity and the Reactivity subscale of the HAS (which assesses self-reported reactivity to stimuli such as bright light and noise) lends support to this proposal. In particular, it indicates that hyperconnectivity among the subnetwork nodes may be the anatomical substrate underlying previous electrophysiological findings in ID including hypersensitivity to sensory stimuli as well as enhanced information processing and attenuated inhibition (Colombo et al., 2016; Perlis et al., 2001; Regestein et al., 1993; Wei et al., 2016, 2018).

Several authors have suggested that the functions of the angular gyrus and its subdivisions need to be understood within the context of their roles among diverse functional networks (Igelström and Graziano, 2017; Seghier, 2013; Zhang and Li, 2014). A number of well-known functional networks including the frontoparietal control

network (FCN), the cingulo-opercular network (CON), the default-mode network (DMN), and the right-lateralized ventral attention network (VAN) contain nodes that overlap with the structural connectivity subnetwork we report here (Igelström and Graziano, 2017). From a cognitive perspective, dysfunctions of the mentioned functional networks appear compatible with the symptomatology of ID. The FCN and CON are instrumental to cognitive control (Power and Petersen, 2013). The DMN usually deactivates during tasks and activates during mind wandering or self-referential processing (Raichle, 2015; Whitfield-Gabrieli and Ford, 2012). The VAN is mainly implicated in shifts of attention due to unexpected stimuli (Corbetta and Shulman, 2002; Vossel et al., 2014). Thus, it may be hypothesized that dyscoordination within and between these functional networks contributes to the hypervigilant psychophysiological profile of people suffering from ID (Bastien, 2011). It must nonetheless be noted that functional and structural connectivity networks denote distinct entities. Functional networks refer to brain areas that consistently coactivate with each other; each of the areas is likely only a subdivision of an anatomical region, and coactivating areas might not be directly connected by white matter tracts. Therefore, it requires future multimodal imaging studies to investigate how structural and functional connectivity properties are related in people with ID.

The fact that deviated subnetwork structural connectivity does not significantly correlate with insomnia duration suggests that connectivity alterations may predispose to ID rather than follow from it. Interestingly, a recent analysis of insomnia-associated genes utilizing the human brain enhancer–gene maps has implicated enriched neural stem cells most significantly at the angular gyrus but also at the caudate nucleus, cingulate gyrus, and hippocampus as well as enriched gene sets related to neuron projection development and neuron maturation at the angular gyrus (Ding et al., 2018). It is thus possible that the alterations we identified have a genetic origin.

Previous studies did not find connectivity strength within the subnetwork anchored at the right angular gyrus to differ between people with ID and matched controls without sleep complaints (Jespersen et al., 2019; Wu et al., 2018). Conversely, these studies reported group differences involving other subnetworks which we did not replicate, even with additional region-of-interest analyses (Supplementary Material). Differences in sample sizes and heterogeneity of the disorder might explain the divergent results. Notably, recently discovered subtypes of ID differ with respect to multiple biologically based cognitive and affective traits (Blanken et al., 2019). Whether or not high scores on a trait (e.g., negative affect) are part of the inclusion or exclusion criteria of a particular study would strongly affect the distribution of subtypes within the sample and, consequently, the sample representation of underlying neural correlates that could be associated with some specific subtypes but not necessarily with the other subtypes. In addition, different imaging protocols and analysis methods could also contribute to inconsistencies. In one study, diffusion-weighted images were acquired with settings similar to ours but on a 1.5-Tesla MRI scanner; deterministic tractography was performed based on the diffusion tensor model (Wu et al., 2018). The method has however been shown to deliver results of low reliability as compared to results obtained from probabilistic tractography based on multi-fiber models such as the one we adopted (Bonilha et al., 2015; Buchanan et al., 2014). The authors also weighted edges by fractional anisotropy, an edge-weighting strategy that could further decrease reliability (Buchanan et al., 2014; Messaritaki et al., 2019). The other study conducted analyses very similar to ours (Jespersen et al., 2019). This study utilized high angular resolution DWI with 71 diffusion gradient directions, which could lead to higher sensitivity to detect other group differences. In particular, although using 32 diffusion gradient directions as we did in the current study is typical for clinical DWI acquisition, it might not fully resolve fiber orientations in brain areas with complex fiber configurations such as the insular region (Ghaziri et al., 2017) where the group differences reported by Jespersen et al. (2019) were primarily located. On the other hand, the strength of the current study is the larger sample size and our verification of the robustness of group differences across a range of edge-weighting strategies.

In conclusion, diffusion tractography reveals brain structural hyperconnectivity in ID within a previously unrecognized subnetwork anchored at the right angular gyrus. The finding is robust across different edge-weighting strategies. Prior knowledge about the functions of the identified subnetwork is compatible with the general characteristics of ID, thus adding to our confidence in the results. Nonetheless, future studies with longitudinal designs and population-based samples are needed to confirm vulnerability of people with strong structural connectivity in the identified subnetwork to the development of ID.

Declaration of Competing Interest

The authors declare that the research was conducted in the absence of any commercial or financial relationships that could be construed as a potential conflict of interest.

Acknowledgments

Research leading to these results has received funding from the Bial Foundation grants 253/12 and 190/16, the Netherlands Organisation of Scientific Research (NWO) grant VICI-453.07.001, the Netherlands Organisation for Health Research and Development (ZonMw) Neuropsychoanalysis Fund 16.561.0001, and the European Research Council Advanced Grant 671084 INSOMNIA.

Supplementary Material

Supplementary material associated with this article can be found, in the online version, at doi:10.1016/j.nicl.2019.102019.

References

Achard, S., Bullmore, E., 2007. Efficiency and cost of economical brain functional networks. PLoS Comput. Biol. 3 (2), e17. https://doi.org/10.1371/journal.pcbi.0030017.

American Academy of Sleep Medicine, 2014. International Classification of Sleep Disorders, 3rd ed. American Academy of Sleep Medicine, Darien, IL.

American Psychiatric Association., 2013. Diagnostic and Statistical Manual of Mental Disorders, 5th ed. American Psychiatric Publishing, Washington, D.C.

Andersen, M.L., Araujo, P., Frange, C., Tufik, S., 2018. Sleep disturbance and pain: a tale of two common problems. Chest 154 (5), 1249–1259. https://doi.org/10.1016/j.chest.2018.07.019.

Andersson, J.L.R., Graham, M.S., Zsoldos, E., Sotiropoulos, S.N., 2016. Incorporating outlier detection and replacement into a non-parametric framework for movement and distortion correction of diffusion MR images. NeuroImage 141, 556–572. https://doi.org/10.1016/j.neuroimage.2016.06.058.

Andersson, J.L.R., Sotiropoulos, S.N., 2016. An integrated approach to correction for off-resonance effects and subject movement in diffusion MR imaging. NeuroImage 125, 1063–1078. https://doi.org/10.1016/j.neuroimage.2015.10.019.

Avants, B.B., Epstein, C.L., Grossman, M., Gee, J.C., 2008. Symmetric diffeomorphic image registration with cross-correlation: evaluating automated labeling of elderly and neurodegenerative brain. Med. Image Anal. 12 (1), 26–41. https://doi.org/10.1016/j.media.2007.06.004.

Avants, B.B., Tustison, N.J., Song, G., Cook, P.A., Klein, A., Gee, J.C., 2011. A reproducible evaluation of ANTs similarity metric performance in brain image registration. NeuroImage 54 (3), 2033–2044. https://doi.org/10.1016/j.neuroimage.2010.09.025.

Bastien, C.H., 2011. Insomnia: neurophysiological and neuropsychological approaches. Neuropsychol. Rev. 21 (1), 22–40. https://doi.org/10.1007/s11065-011-9160-3.

Bastien, C.H., Vallières, A., Morin, C.M., 2001. Validation of the Insomnia Severity Index as an outcome measure for insomnia research. Sleep Med. 2 (4), 297–307. https://doi.org/10.1016/S1389-9457(00)00065-4.

Behrens, T.E.J., Johansen-Berg, H., Jbabdi, S., Rushworth, M.F.S., Woolrich, M.W., 2007. Probabilistic diffusion tractography with multiple fibre orientations: what can we gain? NeuroImage 34 (1), 144–155. https://doi.org/10.1016/j.neuroimage.2006.09.018.

Blanken, T.F., Benjamins, J.S., Borsboom, D., Vermunt, J.K., Paquola, C., Ramautar, J.R., Dekker, K., Stoffers, D., Wassing, R., Wei, Y., Van Someren, E.J.W., 2019. Insomnia disorder subtypes derived from life history and traits of affect and personality. Lancet Psychiatry 6 (2), 151–163. https://doi.org/10.1016/s2215-0366(18)30464-4.

Bonilha, L., Gleichgerrcht, E., Fridriksson, J., Rorden, C., Breedlove, J.L., Nesland, T., Paulus, W., Helms, G., Focke, N.K., 2015. Reproducibility of the structural brain

connectome derived from diffusion tensor imaging. PLoS One 10 (9), e0135247. https://doi.org/10.1371/journal.pone.0135247.
Borsboom, D., Cramer, A.O.J., Schmittmann, V.D., Epskamp, S., Waldorp, L.J., 2011. The small world of psychopathology. PLoS One 6 (11), e27407. https://doi.org/10.1371/journal.pone.0027407.
Buchanan, C.R., Pernet, C.R., Gorgolewski, K.J., Storkey, A.J., Bastin, M.E., 2014. Test–retest reliability of structural brain networks from diffusion MRI. NeuroImage 86, 231–243. https://doi.org/10.1016/j.neuroimage.2013.09.054.
Bullmore, E., Sporns, O., 2009. Complex brain networks: graph theoretical analysis of structural and functional systems. Nat. Rev. Neurosci. 10 (3), 186–198. https://doi.org/10.1038/nrn2575.
Bullmore, E., Sporns, O., 2012. The economy of brain network organization. Nat. Rev. Neurosci. 13 (5), 336–349. https://doi.org/10.1038/nrn3214.
Bzdok, D., Langner, R., Schilbach, L., Jakobs, O., Roski, C., Caspers, S., Laird, A.R., Fox, P.T., Zilles, K., Eickhoff, S.B., 2013. Characterization of the temporo-parietal junction by combining data-driven parcellation, complementary connectivity analyses, and functional decoding. NeuroImage 81, 381–392. https://doi.org/10.1016/j.neuroimage.2013.05.046.
Cappuccio, F.P., D'Elia, L., Strazzullo, P., Miller, M.A., 2010. Quantity and quality of sleep and incidence of type 2 diabetes: a systematic review and meta-analysis. Diabetes Care 33 (2), 414–420. https://doi.org/10.2337/dc09-1124.
Catani, M., Robertsson, N., Beyh, A., Huynh, V., de Santiago Requejo, F., Howells, H., Barrett, R.L.C., Aiello, M., Cavaliere, C., Dyrby, T.B., Krug, K., Ptito, M., D'Arceuil, H., Forkel, S.J., Dell'Acqua, F., 2017. Short parietal lobe connections of the human and monkey brain. Cortex 97, 339–357. https://doi.org/10.1016/j.cortex.2017.10.022.
Chaput, J.-P., Yau, J., Rao, D.P., Morin, C.M., 2018. Prevalence of insomnia for Canadians aged 6 to 79. Health Rep. 29 (12), 16–20.
Colombo, M.A., Ramautar, J.R., Wei, Y., Gómez-Herrero, G., Stoffers, D., Wassing, R., Benjamins, J.S., Tagliazucchi, E., van der Werf, Y.D., Cajochen, C., Van Someren, E.J.W., 2016. Wake high-density electroencephalographic spatiospectral signatures of insomnia. Sleep 39 (5), 1015–1027. https://doi.org/10.5665/sleep.5744.
Corbetta, M., Shulman, G.L., 2002. Control of goal-directed and stimulus-driven attention in the brain. Nat. Rev. Neurosci. 3 (3), 201–215. https://doi.org/10.1038/nrn755.
Dimitriadis, S.I., Drakesmith, M., Bells, S., Parker, G.D., Linden, D.E., Jones, D.K., 2017. Improving the reliability of network metrics in structural brain networks by integrating different network weighting strategies into a single graph. Front. Neurosci. 11, 694. https://doi.org/10.3389/fnins.2017.00694.
Ding, M., Li, P., Wen, Y., Zhao, Y., Cheng, B., Zhang, L., Ma, M., Cheng, S., Liu, L., Du, Y., Liang, X., He, A., Guo, X., Zhang, F., 2018. Integrative analysis of genome-wide association study and brain region related enhancer maps identifies biological pathways for insomnia. Prog. Neuropsychopharmacol. Biol. Psychiatry 86, 180–185. https://doi.org/10.1016/j.pnpbp.2018.05.026.
Dolsen, M.R., Asarnow, L.D., Harvey, A.G., 2014. Insomnia as a transdiagnostic process in psychiatric disorders. Curr. Psychiatry Rep. 16 (9), 471. https://doi.org/10.1007/s11920-014-0471-y.
Edinger, J.D., Bonnet, M.H., Bootzin, R.R., Doghramji, K., Dorsey, C.M., Espie, C.A., Jamieson, A.O., McCall, W.V., Morin, C.M., Stepanski, E.J., 2004. Derivation of research diagnostic criteria for insomnia: report of an American Academy of Sleep Medicine work group. Sleep 27 (8), 1567–1596.
Ghaziri, J., Tucholka, A., Girard, G., Houde, J.-C., Boucher, O., Gilbert, G., ... Nguyen, D.K., 2017. The corticocortical structural connectivity of the human insula. Cereb. Cortex 27 (2), 1216–1228. https://doi.org/10.1093/cercor/bhv308.
Harvey, A.G., Murray, G., Chandler, R.A., Soehner, A., 2011. Sleep disturbance as transdiagnostic: consideration of neurobiological mechanisms. Clin. Psychol. Rev. 31 (2), 225–235. https://doi.org/10.1016/j.cpr.2010.04.003.
He, Q., Zhang, P., Li, G., Dai, H., Shi, J., 2017. The association between insomnia symptoms and risk of cardio-cerebral vascular events: a meta-analysis of prospective cohort studies. Eur. J. Prev. Cardiol. 24 (10), 1071–1082. https://doi.org/10.1177/2047487317702043.
Hertenstein, E., Feige, B., Gmeiner, T., Kienzler, C., Spiegelhalder, K., Johann, A., ... Baglioni, C., 2019. Insomnia as a predictor of mental disorders: a systematic review and meta-analysis. Sleep Med. Rev. 43, 96–105. https://doi.org/10.1016/j.smrv.2018.10.006.
Hunsche, S., Moseley, M.E., Stoeter, P., Hedehus, M., 2001. Diffusion-tensor MR imaging at 1.5 and 3.0 T: initial observations. Radiology 221 (2), 550–556. https://doi.org/10.1148/radiol.2212001823.
Igelström, K.M., Graziano, M.S.A., 2017. The inferior parietal lobule and temporoparietal junction: a network perspective. Neuropsychologia 105, 70–83. https://doi.org/10.1016/j.neuropsychologia.2017.01.001.
Jespersen, K.V., Stevner, A., Fernandes, H., Soerensen, S.D., Van Someren, E.J.W., Kringelbach, M., Vuust, P., 2019. Reduced structural connectivity in insomnia disorder. J. Sleep Res. e12901. https://doi.org/10.1111/jsr.12901. in press.
Jeurissen, B., Descoteaux, M., Mori, S., Leemans, A., 2019. Diffusion MRI fiber tractography of the brain. NMR Biomed. 32 (4), e3785. https://doi.org/10.1002/nbm.3785.
Kyle, S.D., Henry, A.L., 2017. Sleep is a modifiable determinant of health: implications and opportunities for health psychology. Br. J. Health Psychol. 22 (4), 661–670. https://doi.org/10.1111/bjhp.12251.
Li, L., Rilling, J.K., Preuss, T.M., Glasser, M.F., Hu, X., 2012. The effects of connection reconstruction method on the interregional connectivity of brain networks via diffusion tractography. Hum. Brain Mapp. 33 (8), 1894–1913. https://doi.org/10.1002/hbm.21332.
Medaglia, J.D., Lynall, M.-.E., Bassett, D.S., 2015. Cognitive network neuroscience. J. Cogn. Neurosci. 27 (8), 1471–1491. https://doi.org/10.1162/jocn_a_00810.
Messaritaki, E., Dimitriadis, S.I., Jones, D.K., 2019. Assessment of the reproducibility of structural brain networks derived using different edge-weighting strategies. In: Proceedings of the ISMRM 27th Annual Meeting & Exhibition.
Morin, C.M., Drake, C.L., Harvey, A.G., Krystal, A.D., Manber, R., Riemann, D., Spiegelhalder, K., 2015. Insomnia disorder. Nat. Rev. Dis. Prim. 1, 15026. https://doi.org/10.1038/nrdp.2015.26.
Okada, T., Miki, Y., Fushimi, Y., Hanakawa, T., Kanagaki, M., Yamamoto, A., Urayama, S., Fukuyama, H., Hiraoka, M., Togashi, K., 2007. Diffusion-tensor fiber tractography: intraindividual comparison of 3.0-T and 1.5-T MR imaging. Radiology 238 (2), 668–678. https://doi.org/10.1148/radiol.2382042192.
Owen, J.P., Ziv, E., Bukshpun, P., Pojman, N., Wakahiro, M., Berman, J.I., Roberts, T.P.L., Friedman, E.J., Sherr, E.H., Mukherjee, P., 2013. Test–retest reliability of computational network measurements derived from the structural connectome of the human brain. Brain Connect. 3 (2), 160–176. https://doi.org/10.1089/brain.2012.0121.
Park, H.-.J., Friston, K.J., 2013. Structural and functional brain networks: from connections to cognition. Science 342 (6158), 1238411. https://doi.org/10.1126/science.1238411.
Pavlova, M., Berg, O., Gleason, R., Walker, F., Roberts, S., Regestein, Q.R., 2001. Self-reported hyperarousal traits among insomnia patients. J. Psychosom. Res. 51 (2), 435–441. https://doi.org/10.1016/S0022-3999(01)00189-1.
Perlis, M.L., Merica, H., Smith, M.T., Giles, D.E., 2001. Beta EEG activity and insomnia. Sleep Med. Rev. 5 (5), 363–374 S1087079201901510 pii].
Power, J.D., Petersen, S.E., 2013. Control-related systems in the human brain. Curr. Opin. Neurobiol. 23 (2), 223–228. https://doi.org/10.1016/j.conb.2012.12.009.
Raichle, M.E., 2015. The brain's default mode network. Annu. Rev. Neurosci. 38, 433–447. https://doi.org/10.1146/annurev-neuro-071013-014030.
Regestein, Q.R., Dambrosia, J., Hallett, M., Murawski, B., Paine, M., 1993. Daytime alertness in patients with primary insomnia. Am. J. Psychiatry 150 (10), 1529–1534. https://doi.org/10.1176/ajp.150.10.1529.
Riemann, D., Baglioni, C., Bassetti, C., Bjorvatn, B., Dolenc Groselj, L., Ellis, J.G., Espie, C.A., Garcia-Borreguero, D., Gjerstad, M., Gonçalves, M., Hertenstein, E., Jansson-Fröjmark, M., Jennum, P.J., Leger, D., Nissen, C., Parrino, L., Paunio, T., Pevernagie, D., Verbraecken, J., Weeß, H.-G., Wichniak, A., Zavalko, I., Arnardottir, E.S., Deleanu, O.-C., Strazisar, B., Zoetmulder, M., Spiegelhalder, K., 2017. European guideline for the diagnosis and treatment of insomnia. J. Sleep Res. 26 (6), 675–700. https://doi.org/10.1111/jsr.12594.
Roine, T., Jeurissen, B., Perrone, D., Aelterman, J., Philips, W., Sijbers, J., Leemans, A., 2019. Reproducibility and intercorrelation of graph theoretical measures in structural brain connectivity networks. Med. Image Anal. 52, 56–67. https://doi.org/10.1016/j.media.2018.10.009.
Rolls, E.T., Joliot, M., Tzourio-Mazoyer, N., 2015. Implementation of a new parcellation of the orbitofrontal cortex in the Automated Anatomical Labeling atlas. NeuroImage 122, 1–5. https://doi.org/10.1016/j.neuroimage.2015.07.075.
Seghier, M.L., 2013. The angular gyrus: multiple functions and multiple subdivisions. Neuroscientist 19 (1), 43–61. https://doi.org/10.1177/1073858412440596.
Shi, L., Chen, S.-J., Ma, M.-Y., Bao, Y.-P., Han, Y., Wang, Y.-M., Shi, J., Vitiello, M.V., Lu, L., 2018. Sleep disturbances increase the risk of dementia: a systematic review and meta-analysis. Sleep Med. Rev. 40, 4–16. https://doi.org/10.1016/j.smrv.2017.06.010.
Smith, M.T., Huang, M.I., Manber, R., 2005. Cognitive behavior therapy for chronic insomnia occurring within the context of medical and psychiatric disorders. Clin. Psychol. Rev. 25 (5), 559–592. https://doi.org/10.1016/j.cpr.2005.04.004.
Smith, S.M., Jenkinson, M., Woolrich, M.W., Beckmann, C.F., Behrens, T.E.J., Johansen-Berg, H., Bannister, P.R., De Luca, M., Drobnjak, I., Flitney, D.E., Niazy, R.K., Saunders, J., Vickers, J., Zhang, Y., De Stefano, N., Brady, J.M., Matthews, P.M., 2004. Advances in functional and structural MR image analysis and implementation as FSL. NeuroImage 23 (S1), S208–S219. https://doi.org/10.1016/j.neuroimage.2004.07.051.
Sofi, F., Cesari, F., Casini, A., Macchi, C., Abbate, R., Gensini, G.F., 2014. Insomnia and risk of cardiovascular disease: a meta-analysis. Eur. J. Prev. Cardiol. 21 (1), 57–64. https://doi.org/10.1177/2047487312460020.
Sotiropoulos, S.N., Zalesky, A., 2019. Building connectomes using diffusion MRI: why, how and but. NMR Biomed. 32 (4), e3752. https://doi.org/10.1002/nbm.3752.
Tahmasian, M., Noori, K., Samea, F., Zarei, M., Spiegelhalder, K., Eickhoff, S.B., Van Someren, E., Khazaie, H., Eickhoff, C.R., 2018. A lack of consistent brain alterations in insomnia disorder: an activation likelihood estimation meta-analysis. Sleep Med. Rev. 42, 111–118. https://doi.org/10.1016/j.smrv.2018.07.004.
Vossel, S., Geng, J.J., Fink, G.R., 2014. Dorsal and ventral attention systems: distinct neural circuits but collaborative roles. Neuroscientist 20 (2), 150–159. https://doi.org/10.1177/1073858413494269.
Wang, S., Peterson, D.J., Gatenby, J.C., Li, W., Grabowski, T.J., Madhyastha, T.M., 2017. Evaluation of field map and nonlinear registration methods for correction of susceptibility artifacts in diffusion MRI. Front. Neuroinform. 11, 17. https://doi.org/10.3389/fninf.2017.00017.
Wassing, R., Benjamins, J.S., Dekker, K., Moens, S., Spiegelhalder, K., Feige, B., Riemann, D., van der Sluis, S., Van Der Werf, Y.D., Talamini, L.M., Walker, M.P., Schalkwijk, F., Van Someren, E.J.W., 2016. Slow dissolving of emotional distress contributes to hyperarousal. Proc. Natl. Acad. Sci. USA 113 (9), 2538–2543. https://doi.org/10.1073/pnas.1522520113.
Wei, Y., Ramautar, J.R., Colombo, M.A., Stoffers, D., Gómez-Herrero, G., van der Meijden, W.P., te Lindert, B.H.W., van der Werf, Y.D., Van Someren, E.J.W., 2016. I keep a close watch on this heart of mine: increased interoception in insomnia. Sleep 39 (12), 2113–2124. https://doi.org/10.5665/sleep.6308.
Wei, Y., Ramautar, J.R., Colombo, M.A., te Lindert, B.H.W., Van Someren, E.J.W., 2018. EEG microstates indicate heightened somatic awareness in insomnia: toward objective assessment of subjective mental content. Front. Psychiatry 9, 395. https://doi.org/10.3389/fpsyt.2018.00395.
Whitfield-Gabrieli, S., Ford, J.M., 2012. Default mode network activity and connectivity

in psychopathology. Annu. Rev. Clin. Psychol. 8, 49–76. https://doi.org/10.1146/annurev-clinpsy-032511-143049.

Wu, J.Q., Appleman, E.R., Salazar, R.D., Ong, J.C., 2015. Cognitive behavioral therapy for insomnia comorbid with psychiatric and medical conditions: a meta-analysis. JAMA Intern. Med. 175 (9), 1461–1472. https://doi.org/10.1001/jamainternmed.2015.3006.

Wu, Y., Liu, M., Zeng, S., Ma, X., Yan, J., Lin, C., Xu, G., Li, G., Yin, Y., Fu, S., Hua, K., Li, C., Wang, T., Li, C., Jiang, G., 2018. Abnormal topology of the structural connectome in the limbic cortico-basal-ganglia circuit and default-mode network among primary insomnia patients. Front. Neurosci. 12, 860. https://doi.org/10.3389/fnins.2018.00860.

Wulff, K., Gatti, S., Wettstein, J.G., Foster, R.G., 2010. Sleep and circadian rhythm disruption in psychiatric and neurodegenerative disease. Nat. Rev. Neurosci. 11 (8), 589–599. https://doi.org/10.1038/nrn2868.

Zalesky, A., Fornito, A., Bullmore, E.T., 2010. Network-based statistic: identifying differences in brain networks. NeuroImage 53 (4), 1197–1207. https://doi.org/10.1016/j.neuroimage.2010.06.041.

Zhang, S., Li, C.-S.R., 2014. Functional clustering of the human inferior parietal lobule by whole-brain connectivity mapping of resting-state functional magnetic resonance imaging signals. Brain Connect. 4 (1), 53–69. https://doi.org/10.1089/brain.2013.0191.